Comparison Between In Situ Hybridization and Real-time PCR Technique as a Means of Detecting the Integrated Form of Human Papillomavirus 16 in Cervical Neoplasia

Takuma Fujii, MD, Nobuo Masumoto, MD,* Miyuki Saito, CT,* Nobumaru Hirao, MD,* Shinichi Niimi, PhD,† Makio Mukai, MD,‡ Akiko Ono, MD,* Shigenori Hayashi, MD,* Kaneyuki Kubushiro, MD,* Eiichi Sakai, PhD,† Katsumi Tsukazaki, MD,* and Shiro Nozawa, MD**

Abstract: Integration of the human papillomavirus (HPV) genome is thought to be one of the causes of cancer progression. However, there is controversy concerning the physical status of HPV 16 in premalignant cervical lesions, and there have been no reports on the concordance between detection of the integrated form of HPV16 by real-time PCR and by in situ hybridization. We investigated specimens of cervical intraepithelial neoplasia (CIN) and invasive carcinomas for the physical status of HPV 16 by real-time PCR and in situ hybridization. The presence of the integrated form was detected by both real-time PCR and in situ hybridization in zero of four cases of CIN1, three of six cases of CIN2, nine of 27 cases of CIN3, and two of six cases of invasive carcinomas. Integrated HPV 16 was present in some premalignant lesions but was not always present in carcinomas. The concordance rate between the two methods for the detection of the presence of the integrated form was 37 of 43 (86%) cases. Real-time PCR and in situ hybridization were found to be complementary and convenient techniques for determining the physical status of the HPV genome. We conclude that a combination of both methods is a more reliable means of assessing the physical status of the HPV genome in cervical neoplasia.

Key Words: human papillomavirus, real-time PCR, in situ hybridization, integration, cervical neoplasia

(*Diagn Mol Pathol* 2005;14:103–108)

Human papillomavirus (HPV) DNA is found in more than 90% of cervical carcinomas,[1] and HPV16 has been reported to be the dominant type of HPV in cervical carcinomas. Detection of HPV16 is proportional to the degree of cervical neoplasia: HPV16 has been detected in 15% of cervical intraepithelial neoplasia (CIN) 1, 30% of CIN2, and 50% of CIN3 and invasive carcinomas.[2,3] Integration of the HPV genome is thought to be one of the causes of cancer progression. Viral DNA that has been integrated into the host genome disrupts some early genes, such as the E1 and E2 open reading frames (ORFs), whereas the E6 and E7 ORFs remain intact. E6 protein binds to and degrades the tumor suppressor P53 protein via ubiquitin pathways.[4] E7 protein binds to the tumor suppressor Rb protein followed by E2F, transcriptional factor, compelled the cell-cycle rotation.[5] Münger reported that E7 protein is capable of causing aneuploidy in stratified squamous cells.[6] E7 protein plays an important role in the onset of dysplastic change, and the level of the expression of E7 protein may depend on the physical status of the HPV genome in cells. In an in vitro study, Lambert found that the integration of HPV16 results in an increase in E7 transcripts in cultured cells.[7] Thus, it is very important to determine the status of HPV16 genome in cervical neoplasia to elucidate the mechanisms of cervical cancer. In a study by real-time PCR, Peitsaro showed that integration had occurred in 23 of 24 premalignant lesions in patients with HPV16 infection.[8] By contrast, Southern blot analysis has shown that some cervical cancers contain the episomal form,[9,10] and thus there is still controversy concerning the physical status of the HPV16 genome in premalignant lesions and carcinomas of the cervix.[11–13] We realize that Southern blot analysis is the most reliable method of determining whether the integrated form is present in a specimen, but this analysis was not used in this study because only very small specimens were harvested from the premalignant lesions. By contrast, real-time PCR and in situ hybridization technique have been reported to be useful for investigating the physical status of the HPV genome in premalignant and cancerous specimens.[8,14–20] The question then arises as to the validity and concordance of real-time PCR and in situ hybridization. The purpose of this study was to assess the physical status of the HPV genome and to determine the degree of agreement between the results obtained by these two methods.

MATERIALS AND METHODS

Specimen and Sample Preparation

Patients diagnosed with cervical neoplasia on the basis of the results of biopsies performed during colposcopy at Keio University Hospital, in Tokyo, Japan, between October 2000 and April 2001 were enrolled in the study. Exfoliated cells into ThinPrep vials were collected with a broom device (Cervex Brush; Unimar, Wilton) just before colposcopy and then stored at ambient temperature, to be used for the HPV-DNA analysis

From the *Department of Obstetrics and Gynecology, Keio University School of Medicine, Tokyo, Japan; †Nihon Gene Research Laboratories Inc., Sendai City, Japan; and ‡Department of Pathology, Keio University School of Medicine, Tokyo, Japan.

Supported by a Grand-in-Aid for Scientific Research (C) and (A) Japan Society for the Promoter of Science and Research Grants for Life Science and Medicine, and the Keio University Medical Science Fund.

Reprints: Takuma Fujii, Department of Obstetrics and Gynecology, Keio University, School of Medicine, Shinanomachi 35, Shinjuku-ku, Tokyo 160-8582, Japan (e-mail: fujii@sc.itc.keio.ac.jp).

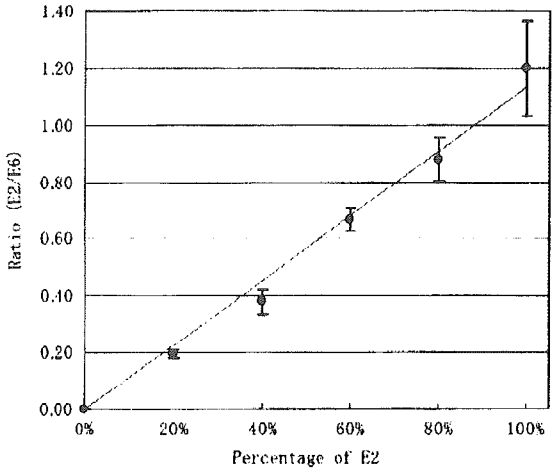

FIGURE 1. Control experiment using real-time quantitative PCR with the LightCycler system: the PCRE67 plasmid was mixed with a PK114/K plasmid to prepare a mixture of HPV 16 DNA. The PK114/K plasmid was replaced by an equivalent copy number of the PCRE67 plasmid in increments of 20%. DNA solutions containing episomal DNA (PK114/K exclusively), integrated DNA (pCRE67 exclusively), and a mixture form of HPV 16 DNA (20%-80% integrated) were prepared. The E2 and E6 copy number was quantitatively determined 6 times by real-time PCR assay, and the ratio of the E2 copy number to E6 copy number was calculated for each DNA solution. The cutoff value to distinguish the mixed form from the pure episomal form was set at 0.79. Details of calculation are described in the text.

within 12 months of collection. To perform the analysis, approximately 10 mL of preserved fluid from ThinPrep vials was centrifuged at 3,000 rpm for 30 minutes, and after washing the pellet once in phosphate-buffered saline, genomic DNA was extracted with proteinase K and phenol-chloroform. The quality and quantity of the extracted genomic DNA were monitored by ethidium-bromide– stained agarose gel electrophoresis. HPV DNA was identified by PCR analysis with consensus primer pairs designed to amplify an approximately 250-bp segment of HPV DNA.[21] These consensus primer pairs target the HPV L1 ORF and detect a broad range of genital HPVs. HPV typing and sequencing analysis were performed in all PCR-positive cases.[3]

Real-Time PCR

To generate a pCR-TOPO E6/E7 plasmid (designated PCRE67 plasmid) which contains the E6 gene and E7 gene, a PK114/K plasmid containing a variant HPV16 genome, was amplified by PCR and introduced into the cloning site (Invitrogen, San Diego, CA). The primers for PCR amplification were as follows: E6/E7F, 5′-ATGTTTCAGGACCCACAGGAG-3′ (104-124) and E6/E7R, 5′-GGTAGATTATGGTTTCTGA-GA-3′ (844-864). The PK114/K plasmid contains one copy each of the E2 and E6 ORFs, whereas the PCRE67 plasmid carried the entire E6 ORF but lacked the E2 ORF. The PCRE67 plasmid was mixed with the PK114/K to prepare a mixture of the episomal form and the integrated form of HPV 16 DNA. The PK114/K was replaced by an equivalent copy number of the PCRE67 plasmid in increments of 20% to prepare DNA solutions containing the episomal form of HPV16 DNA (PK114/K exclusively), the integrated form of HPV16 DNA (PCRE67 exclusively), and both forms of HPV 16 DNA (20%-80% integrated form). The E2 and E6 copy numbers were quantitatively determined six times by real-time PCR, and the

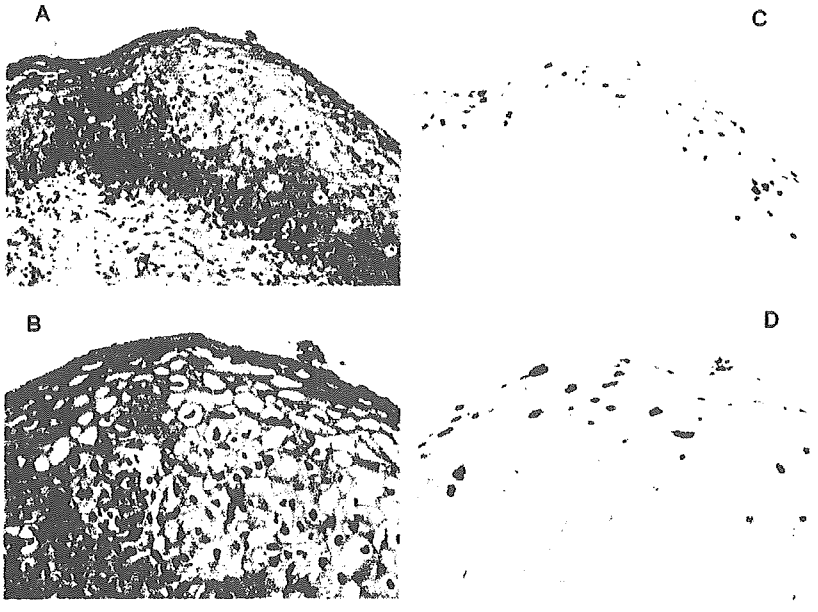

FIGURE 2. Case 3325, representative of the diffuse pattern: hematoxylin and eosin-stained section (A, ×20; B, ×40). In situ hybridization with the diffuse pattern (D) with the HPV16 probe (C, ×20; D, ×40).

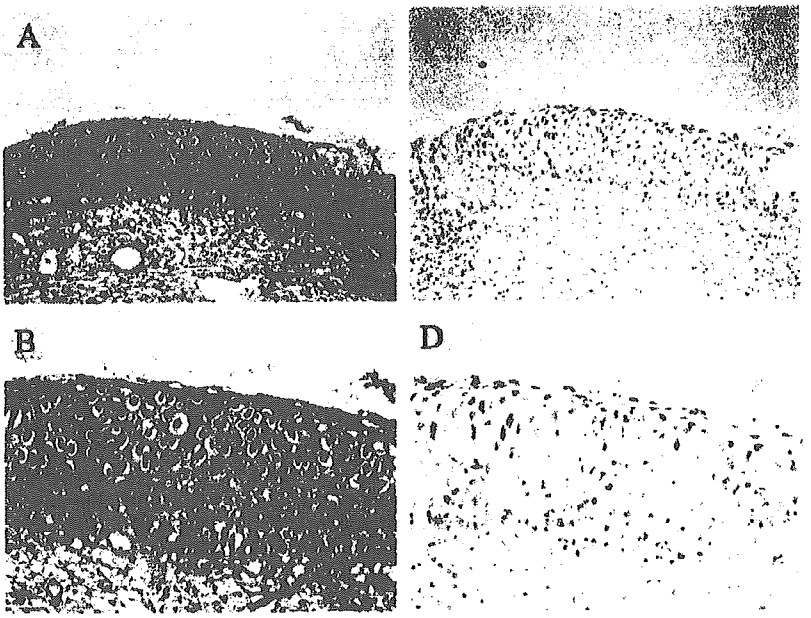

FIGURE 3. Case 613, representative of the spot pattern: hematoxylin and eosin-stained section (A, ×20; B, ×40). In situ hybridization with the spot pattern (S) with the HPV16 probe (C, ×20; D, ×40).

ratio of the E2 copy number to the E6 copy number was calculated for each DNA solution. Differences in ratio between the episomal form and other forms (pure integrated and mixed forms) were analyzed by the unpaired *t* test. Probability values less than 0.01 were considered statistically significant. Real-time PCR was performed with the LightCycler (Roche Diagnostics, Germany) system. PCR for the HPV-16 E2 gene was performed with 2 μL of master mix (LightCycler FastStart DNA Master Hybridization Probes, Roche Diagnostics) containing buffer, dATP, dCTP, dGTP, dUTP, Taq polymerase, 3 mmol/L $MgCl_2$, 0.2 μmol/L probe (Nihon Gene Research Laboratories, Japan), 0.6 μmol/L forward primer, 0.5 μmol/L reverse primer (Nihon Gene Research Laboratories Inc, Japan), a template DNA, and water added to a final volume of 20 μL. PCR for the HPV-16 E6 gene was performed with 2 μL of master mix (LightCycler FastStart DNA Master Hybridization Probes, Roche Diagnostics) containing buffer, dATP, dCTP, dGTP, dUTP, Taq polymerase, 4 mmol/L $MgCl_2$, 0.2 μmol/L probe (Nihon Gene Research Laboratories, Japan), 0.5 μmol/L of each primer (Nihon Gene Research Laboratories Inc, Japan), a template DNA, and water added to a final volume of 20 μL. The PCR cycle for the E2 and E6 gene included denaturation at 95°C for 10 seconds, annealing and extension 60°C for 25 seconds, and cooling at 40°C for 30 seconds, followed by 45 cycles of amplification. The primers used for PCR of the E2 gene were as follows: forward, 5′-TGTGTTTAGCAGCAACGAAG-3′ (3349-3368) and reverse, 5′-GCTGGATAGTCGTCTGTGTT-3′ (3454-3473). The probe was FAM-5′ CAAGGCGACGGCTTTGGTATGGGTC-3′-TAMRA (3418-3442). The primers used for PCR of the E6 gene were as follows: forward, 5′-CGACCCAGAAAGT-TACCA-3′ (125-142) and reverse, 5′-AGCAAAGTCATATA-CCTCACG-3′ (220-241). The probe used was FAM-5′ TTAT-GCACAGAGCTGCAAACAACTATACATGA-3′-TAMRA (146-177). Two standard curves were obtained by amplification of dilution series of 10^2 to 10^7 copies of the PK114/k plasmid.

TABLE 1. Concordance Between the Physical Status of the HPV Genome According to the Results of Real-time PCR and In Situ Hybridization

		ISH				
	PCR	D	DS	S	Absence	Total
CIN I	Integration pattern					
	Presence	0	0	0	0	0
	Absence	1	0	0	3	4
CIN II	Integration pattern					
	Presence	0	2	1	1*	4
	Absence	2	0	0	0	2
CIN III	Integration pattern					
	Presence	3*	3	6	0	12
	Absence	5	0	2*	8	15
MIC	Integration pattern					
	Presence	0	0	1	0	1
	Absence	1	0	0	2	3
SCC	Integration pattern					
	Presence	0	0	1	0	1
	Absence	0	0	0	1	1
Total						43

*Indicates discrepancies between the two methods.
MIC, microinvasive carcinomas; SCC, squamous cell carcinomas.
The shadow box represents the concordance between the results of the two methods for the presence of the integrated form.

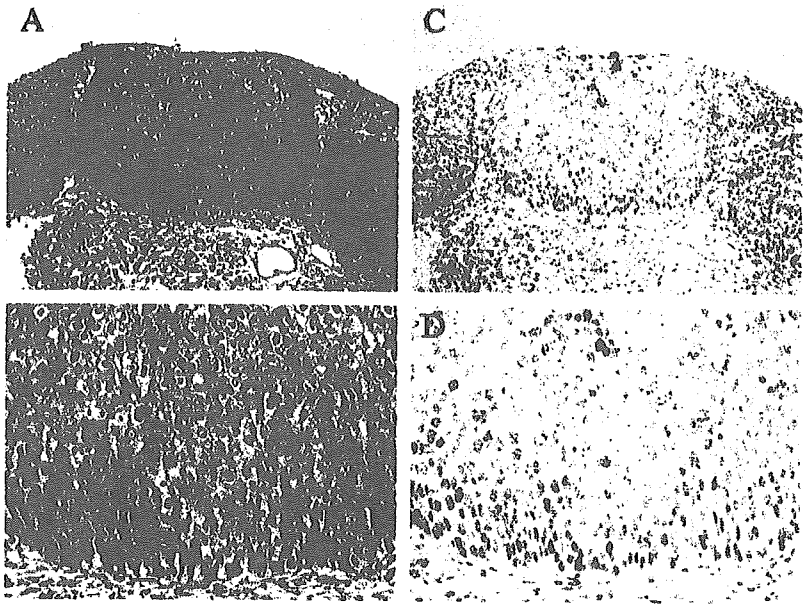

FIGURE 4. Case 91, representative of the diffuse and spot pattern: hematoxylin and eosin-stained section (A, ×20; B, ×40). In situ hybridization with the diffuse and spot pattern (DS) with the HPV16 probe (C, ×20; D, ×40).

In Situ Hybridization

In situ hybridization was carried out with the GenPoint kit catalyzed signal amplification system (Dako Cytomation, Kyoto, Japan) as described in the instruction manual. Briefly, formalin-fixed, paraffin-embedded tissue slides were deparaffinized, pretreated with Target Retrieval Solution at 95°C for 40 minutes, and then exposed to proteinase K diluted 1:6,000 to 1:10,000 at room temperature for 10 minutes. The tissue slides were then soaked in 0.3% hydrogen peroxide in methanol at room temperature for 20 minutes, dehydrated through a graded alcohol series, and air dried. The biotin-labeled HPV16 probe was then applied to the tissue slides. After denaturing at 95°C for 5 minutes and hybridization at 37°C overnight, the tissue slides were washed in Stringent Wash Solution at 45°C or 55°C for 20 minutes and rinsed in Tris buffered saline with Tween 20 (TBST). The tissue slides were then incubated with 1:100 diluted horseradish peroxidase-conjugated streptavidin at room temperature for 15 minutes. After rinsing with TBST three times, the slides were incubated with biotinyl tyramine at room temperature for 15 minutes, and after washing the slides with TBST three times, they were incubated with horseradish peroxidase-conjugated streptavidin at room temperature for 15 minutes and washed three times in TBST. For signal development, 3, 3′-diaminobenzidine tetrahydrochloride was used as the substrate, and positive signals were detected in the form of a brown color under a light microscope. The sections were weakly counterstained with hematoxylin. The signal types were assessed as described previously.[22–24] Diffuse (D) signals, defined as diffuse positivity throughout the nuclei, were reported as the episomal form, Spot (S) signals localized in the nuclei, as the integrated form, and both diffuse and spot (DS) signals as a combination of the episomal form and the integrated form.

RESULTS

The Presence of the Integrated Form by Real-Time PCR

We examined 3,000 specimens of exfoliated cervical cells obtained from cervical cancer screening and investigated the 43 specimens in which HPV16 had already been identified by PCR followed by direct sequencing.[3] It is possible to investigate whether the integrated form is present or not by comparing the E2/E6 ratios by real-time PCR. In other words, if only the episomal form were present, the E2/E6 ratios would be almost the same, and if only the integrated form were present, the E2/E6 ratios would be very low. If the integrated form and episomal form were mixed, the E2/E6 ratios would be intermediate between the values for the pure episomal form and the integrated form. We therefore conducted the analysis in the assessment by real-time PCR in our study to determine whether the integrated form was present by examining the E2/E6 ratios. We set the cutoff value to distinguish the mixed episomal and integrated form from the pure episomal form was set at 0.79. The basis for setting the cutoff value at 0.79 is that we measured the E2/E6 ratio six times in a control experiment, and when we computed the mean and standard deviation and then calculated the 99% confidence interval, we obtained an interval of 0.79 to 1.61. Thus, if the E2/E6 ratio were less than 0.79, the chance of being the pure episomal form would be less than 1%, namely, integrated HPV16 DNA was therefore

considered to be present when the E2/E6 copy number ratio was below 0.79 (Fig. 1). Integrated DNA was found to be present in none of the four CIN1 cases, four of the six (66%) CIN2 cases, and 12 of the 27(44%) CIN3 cases. There were no significant differences between the CIN2 and CIN3 cases in percentage of positive cases, suggesting that integration may occur in the stage of CIN2. We also investigated six squamous cell carcinomas, consisting of microinvasive carcinomas and invasive squamous cell carcinomas, and two contained the integrated form (Table 1).

Detection of the Integrated Form by In Situ Hybridization

One of four CIN1 cases yielded D signals, indicating the presence of the episomal form (Fig. 2). Five of the six CIN2 cases of yielded positive signals, and three (50%) yielded DS or S signals, indicating the presence of the integration. Twelve of 27 CIN3 cases yielded positive signals, and 9 (33%) yielded DS or S signals (Figs. 3 and 4). Investigation of six squamous cell carcinomas yielded S signals in two (33%), D signals in one, and DS signals in none (Table 1).

Concordance Between the Results for the Detection of the Integrated Form by Real-Time PCR and by In Situ Hybridization

We compared the results of detection about the integrated form by both real-time PCR and in situ hybridization. The integrated form was not detected in CIN1 by either real-time PCR or in situ hybridization. In CIN2, both methods identified the integrated form in three (50%) of the six cases, and they identified the integrated form in nine (33%) of the 27 CIN3 cases. Although there was some difference between the results obtained by the two methods, the concordance rate for detection of the integrated form was 37 of 47 (86%) in Table 1. Thus, the results of the two methods for detection of the integrated form almost always agreed.

DISCUSSION

HPV18 and HPV33 have been found in cervical carcinomas in their integrated forms, whereas HPV16 has been found in the pure integrated, the pure episomal form, or the mixed form. It is noteworthy that the physical status of HPV16 in cervical neoplasia is unique.[25,26] We therefore used real-time PCR and in situ hybridization to investigate whether cervical neoplasia contains the integrated form of the HPV16 genome. Real-time PCR has recently been used to determine the physical status of the HPV genome, and it has the advantage of being sensitive enough to use in small amount of samples. The template DNA can be obtained from exfoliated cervical cells preserved for liquid cytology, however, there has been a great deal of criticism of determination of the physical status of the HPV genome by real-time PCR. Since we selected the E2 and E6 regions for real-time PCR primers to compare differences in DNA amplification between the E2 and E6 ORFs, the physical status of the genome may have been misinterpreted based on the results. It is known to be limited discussion regarding the physical status only by real-time PCR. However, since there have been many reports that the E2 is most often disrupted when viral DNA is integrated into the host genome, we assessed the detection of the integrated form based on the E2/E6 ratio according to the results of real-time PCR. It is noteworthy that the incidence of integration was not as high as previously reported on the basis of real-time PCR.[8] We assume that the discrepancy is due to the cutoff values used in the control experiments.

Since the physical status of the HPV genome has also recently been investigated by in situ hybridization, we used in situ hybridization as an alternative assay for detection of the integrated form for comparison. The greatest advantage of in situ hybridization is that neoplastic area and nonneoplasite area of the same specimen can be examined by microscopy for positive signals. The in situ hybridization system used in our study was based on catalyzed amplification of positive hybridization signals with biotin tyramide complexes and does not require PCR amplification to improve sensitivity. Nevertheless, its sensitivity appeared to be poorer to that of the PCR technique, and that presumably explains the failure to detect positive signals in the CIN 1 (Table 1). Evans et al[15] reported detection of spot signals in 100% of CIN by in situ hybridization, but they observed spot signals even in low risk of HPVs genome such as HPV 6 or 11 under their conditions. There is controversy as to whether low-risk HPV is integrated into the host genome or not. Under the present circumstances, in which the low-risk type has not generally been recognized as being present as the integrated form, we should consider the sensitivity and specificity of their assay. Since the results obtained with our high-sensitivity in situ hybridization almost completely coincided with the results of real-time PCR, we concluded that our assay more closely reflects reality.

The discrepancy between the results obtained by two methods in our study may be due to the difference between the samples. Exfoliated cells were investigated by real-time PCR, whereas biopsy material was examined by in situ hybridization. Despite the difference in such an experimental condition, we found strong concordance between the results of real-time PCR and in situ hybridization. We conclude that a combination of real-time PCR and in situ hybridization is a more reliable method than using either method alone to determine the physical status of the HPV genome.

We also investigated the physical status of the HPV genome in our specimens and the clinical outcome of the patients. The group with having the integrated pattern tended to show persistent HPV infection; however, in these cases, laser vaporization was performed during the observation period at the patients' request (data not shown). Therefore, we could not conclude that integration is an indicator of a poor outcome. Although the lesions regressed spontaneously in most CIN2 cases, the integrated form was found in some CIN2 cases. It remains unresolved whether the presence of the integrated form is an indicator of progression of cervical neoplasia because the integrated form was not detected in all of the invasive carcinomas. From the standpoint of the gynecologic oncologist, the CIN classification still seems to be the ordinary international terminology for histologic diagnosis. Our data have demonstrated that the pattern of HPV gene presence is different in the CIN1 group and the CIN2 group. In other words, they clearly show that CIN1, ie, low-grade squamous

intraepithelial lesions (LSILs), differ from CIN2 or higher-grade lesions, ie, high-grade squamous intraepithelial lesions (HSILs), biologically as well. If it is found that SIL, which is generally used in cytologic terminology, is theoretically consistent from a molecular biology standpoint as well, it seems that the concept of SIL will be widely recognized in the future as histologic terminology. We feel that our study is important from this viewpoint as well. On the other hand, since clinical regression also occurs in many CIN2 cases, there is a problem in deciding on CIN2 and higher-grade cases as targets for treatment. Differentiating between CIN2 and CIN3 is important in terms of deciding on treatment policy. Thus, at the present time making a histologic diagnosis into just two groups, an LSIL group and an HSIL group, is difficult for clinicians to accept. That is why we used the biopsy samples and the CIN classification to describe them in the present study. The incidence of anti E7 antibody in cervical neoplasia patients has been reported to be 20% to 50%,[27,28] but the relationship between E7 expression in cells and the incidence of anti E7 antibody remains unresolved. If production of anti E7 antibody in cervical neoplasia patients is related to the physical status of the HPV genome, it might be useful to work out a strategy for therapeutic vaccination for the E7 protein in the future.

ACKNOWLEDGMENTS

We are grateful to Dr. Iwata for discussions. The authors thank Dr. Mattias Durst for the gift of the PK114/K plasmid containing the variant HPV16 genome.

REFERENCE

1. zur Hausen H. Viruses in human cancers. *Science*. 1991;254:1167–1173.
2. Nakagawa H, Sugano K, Fujii T, et al. Frequent detection of human papilloma viruses in cervical dysplasia by PCR single-strand DNA-conformational polymorphism analysis. *Anticancer Res*. 2002;22:1655–1660.
3. Masumoto N, Fujii T, Ishikawa M, et al. Papanicolaou tests and molecular analyses using new fluid-based specimen collection technology in 3000 Japanese women. *Br J Cancer*. 2003;88:1883–1888.
4. Scheffner M, Nuber U, Huibregtse JM. Protein ubiquitination involving an E1-E2-E3 enzyme ubiquitin thioester cascade. *Nature*. 1995;373:81–83.
5. Nevins JR. E2F: A link between the Rb tumor suppressor protein and viral oncoproteins. *Science*. 1992;258:424–429.
6. Duensing S, Duensing A, Flores ER, et al. Centrosome abnormalities and genomic instability by episomal expression of human papillomavirus type 16 in raft cultures of human keratinocytes. *J Virol*. 2001;75:7712–7716.
7. Jeon S, Allen-Hoffmann BL, Lambert PF. Integration of human papillomavirus type 16 into the human genome correlates with a selective growth advantage of cells. *J Virol*. 1995;69:2989–2997.
8. Peitsaro P, Johansson B, Syrjanen S. Integrated human papillomavirus type 16 is frequently found in cervical cancer precursors as demonstrated by a novel quantitative real-time PCR technique. *J Clin Microbiol*. 2002;40:886–891.
9. Matsukura T, Koi S, Sugase M. Both episomal and integrated forms of human papillomavirus type 16 are involved in invasive cervical cancers. *Virology*. 1989;172:63–72.
10. Durst M, Kleinheinz A, Hotz M, et al. The physical state of human papillomavirus type 16 DNA in benign and malignant genital tumours. *J Gen Virol*. 1985;66:1515–1522.
11. Klaes R, Woerner SM, Ridder R, et al. Detection of high-risk cervical intraepithelial neoplasia and cervical cancer by amplification of transcripts derived from integrated papillomavirus oncogenes. *Cancer Res*. 1999;59:6132–6136.
12. Luft F, Klaes R, Nees M, et al. Detection of integrated papillomavirus sequences by ligation-mediated PCR (DIPS-PCR) and molecular characterization in cervical cancer cells. *Int J Cancer*. 2001;92:9–17.
13. Gallo G, Bibbo M, Bagella L, et al. Study of viral integration of HPV-16 in young patients with LSIL. *J Clin Pathol*. 2003;56:532–536.
14. Nagao S, Yoshinouchi M, Miyagi Y, et al. Rapid and sensitive detection of physical status of human papillomavirus type 16 DNA by quantitative real-time PCR. *J Clin Microbiol*. 2002;40:863–867.
15. Evans MF, Mount SL, Beatty BG, et al. Biotinyl-tyramide-based in situ hybridization signal patterns distinguish human papillomavirus type and grade of cervical intraepithelial neoplasia. *Mod Pathol*. 2002;15:1339–1347.
16. Birner P, Bachtiary B, Dreier B, et al. Signal-amplified colorimetric in situ hybridization for assessment of human papillomavirus infection in cervical lesions. *Mod Pathol*. 2001;14:702–709.
17. Ueda Y, Enomoto T, Miyatake T, et al. Monoclonal expansion with integration of high-risk type human papillomaviruses is an initial step for cervical carcinogenesis: Association of clonal status and human papillomavirus infection with clinical outcome in cervical intraepithelial neoplasia. *Lab Invest*. 2003;83:1517–1527.
18. Cooper K, Herrington CS, Stuckland JE, et al. Episomal and integrated human papillomavirus in cervical neoplasia shown by non-isotopic in situ hybridisation. *J Clin Pathol*. 1991;44:990–996.
19. Huang CC, Kashima ML, Chen H, et al. HPV in situ hybridization with catalyzed signal amplification and polymerase chain reaction in establishing cerebellar metastasis of a cervical carcinoma. *Hum Pathol*. 1999;30:587–591.
20. Lizard G, Demares-Poulet MJ, Roignot P, et al. In situ hybridization detection of single-copy human papillomavirus on isolated cells, using a catalyzed signal amplification system: GenPoint. *Diagn Cytopathol*. 2001;24:112–116.
21. Yoshikawa H, Kawana T, Kitagawa K, et al. Detection and typing of multiple genital human papillomaviruses by DNA amplification with consensus primers. *Jpn J Cancer Res*. 1991;82:524–531.
22. Masumoto N, Fujii T, Ishikawa M, et al. P16 overexpression and human papillomavirus infection in small cell carcinoma of the uterine cervix. *Hum Pathol*. 2003;34:778–783.
23. Cooper K, Herrington CS, Graham AK, et al. In situ human papillomavirus (HPV) genotyping of cervical intraepithelial neoplasia in South African and British patients: Evidence for putative HPV integration in vivo. *J Clin Pathol*. 1991;44:400–405.
24. Conger KL, Liu JS, Kuo SR, et al. Human papillomavirus DNA replication. Interactions between the viral E1 protein and two subunits of human DNA polymerase alpha/primase. *J Biol Chem*. 1999;274:2696–2705.
25. Kristiansen E, Jenkins A, Holm R. Coexistence of episomal and integrated HPV16 DNA in squamous cell carcinoma of the cervix. *J Clin Pathol*. 1994;47:253–256.
26. Pirami L, Giache V, Becciolini A. Analysis of HPV16, 18, 31, and 35 DNA in pre-invasive and invasive lesions of the uterine cervix. *J Clin Pathol*. 1997;50:600–604.
27. Meschede W, Zumbach K, Braspenning J, et al. Antibodies against early proteins of human papillomaviruses as diagnostic markers for invasive cervical cancer. *J Clin Microbiol*. 1998;36:475–480.
28. Fujii T, Matsushima Y, Yajima M, et al. Serum antibody against unfused recombinant E7 protein of human papillomavirus type 16 in cervical cancer patients. *Jpn J Cancer Res*. 1995;86:28–34.

Available online at www.sciencedirect.com

SCIENCE DIRECT

Gynecologic Oncology 98 (2005) 453–461

Gynecologic Oncology

www.elsevier.com/locate/ygyno

Transcriptional expression of the genes implicated in angiogenesis and tumor invasion in cervical carcinomas

Koji Kanda, Masatsugu Ueda*, Hikari Futakuchi, Hiroyuki Yamaguchi, Kuniko Mori, Yoshito Terai, Minoru Ueki

Department of Obstetrics and Gynecology, Osaka Medical College, 2-7 Daigakumachi, Takatsuki, Osaka 569-8686, Japan

Received 10 February 2005
Available online 5 July 2005

Abstract

Objective. Co-expression patterns of the genes implicated in angiogenesis and tumor invasion in cervical carcinoma cells were investigated together with invasive activity of tumor cells. Transcript levels of those genes were also compared between tumor cells and normal cervical tissues.

Methods. Real-time quantitative RT-PCR analysis was conducted on selected 11 genes (total VEGF-A, $VEGF_{121}$, $VEGF_{165}$, $VEGF_{189}$, VEGF-B, C and D, bFGF, dThdPase, MMP-2 and uPA) using 11 cervical carcinoma cell lines and 14 normal cervical tissues. Protein expression of VEGF-C and MMP-2 and invasive activity of tumor cells were evaluated for each cell line by sandwich ELISA and haptoinvasion assay, respectively.

Results. Gene co-expression analysis revealed the significant correlation between angiogenic factors and proteinases in malignant but not in normal cervical samples. Gene or protein expression levels of VEGF-C and MMP-2 were well correlated with the number of invaded tumor cells. VEGF-A splicing variants were increased in malignant compared to normal cervical samples but not associated with the invasive activity of the cells.

Conclusion. VEGF-C and MMP-2 were closely related to invasive phenotype of tumor cells, whereas VEGF-A isoforms were considered to be involved in cervical carcinogenesis.

Keywords: Angiogenesis; Invasion; VEGF-C; MMP-2; Cervical carcinoma

Introduction

Growth of solid tumors depends on angiogenesis, the process by which new blood vessels develop from the endothelium of a pre-existing vasculature [1]. Tumors promote angiogenesis by secreting various angiogenic factors, and newly formed blood vessels induce tumor cell proliferation and invasiveness. Various peptide growth factors, such as vascular endothelial growth factor (VEGF) [2,3], basic fibroblast growth factor (bFGF) [4,5] and thymidine phosphorylase (dThdPase) [6–8], have been found to stimulate the proliferation and motility of endothelial cells, thus inducing new blood vessel formation. Molecular cloning has revealed five different isoforms of VEGF-A which are generated from a single mRNA by alternative splicing and which have different biochemical features and biological effects [9,10]. Recently, three new members of the VEGF family, VEGF-B, C and D, have been also discovered and characterized [11–13]. It has been suggested that VEGF family members, bFGF and dThdPase, are expressed in a variety of human tumors in different ways.

Metastatic spread of the solid tumor depends on a critical cascade of events that includes tumor cell adhesion, migration, invasion, proliferation and ultimately neovascularization [14]. These biological processes require

* Corresponding author. Fax: +81 72 681 3723.
E-mail address: gyn017@poh.osaka-med.ac.jp (M. Ueda).

0090-8258/$ - see front matter © 2005 Elsevier Inc. All rights reserved.
doi:10.1016/j.ygyno.2005.05.005

proteolysis for degradation of extracellular matrices (ECM). This allows tumor cells to invade through tissue stroma and subsequently to enter and spread via the blood and lymphatic systems. Matrix metalloproteinases (MMPs), including MMP-2 and 9 (gelatinase A and B), are members of proteolytic enzymes which can degrade native collagens and other ECM components [15]. Enhanced mRNA and protein levels of MMP-2 and/or 9 have been detected in a variety of human malignant tumors. It is also noted that the urokinase-type plasminogen activator (uPA) plays an important role in the invasion process [16]. The proteolytic cascade of ECM components is triggered by the uPA-mediated conversion of plasminogen to plasmin and the subsequent activation of procollagenases [17].

The primary tumor with a high proportion of angiogenic cells is likely to give rise to metastatic implants that are already angiogenic, enabling them to grow in lymphnodes and distant organs [18]. Tumors that produce a higher level of angiogenic factors may have a more aggressive behavior than tumors negative for those factors in the process of invasion and metastasis. It may be expected that the expression of various angiogenic factors in tumor cells is closely associated with invasive phenotype of the cells. However, there have been very few reports on the co-expression patterns of the genes implicated in angiogenesis and tumor invasion [19].

In the present study, we investigated gene or protein expression levels of various angiogenic factors and proteolytic enzymes in cervical carcinoma cells and correlated them with invasive activity of the cells. Moreover, we sought to determine whether a different co-expression pattern of those genes exists between tumor cells and normal cervical tissues.

Materials and methods

Cell culture

Experiments were conducted using seven human cervical squamous cell carcinoma (SKG-I, SKG-II, SKG-IIIa, SKG-IIIb, OMC-1, YUMOTO and QG-U) and four adenocarcinoma (HOKUG, NUZ, OMC-4 and CAC-1) cell lines. The OMC-1 [20] and OMC-4 [21] cell lines were established in our laboratory. The SKG-I [22], SKG-II [23], SKG-IIIa and SKG-IIIb [24] cell lines were kindly provided by Dr. Shiro Nozawa, Keio University, Tokyo. The YUMOTO [25], QG-U [26] and NUZ [27] cell lines were kindly provided by Dr. Naotake Tanaka, Chiba University, Chiba. The HOKUG [28] and CAC-1 [29] cell lines were provided by Dr. Isamu Ishiwata, Ishiwata Hospital, Mito and Dr. Osamu Hayakawa, Sapporo Medical College, Sapporo, respectively. All of the 11 cell lines, except for the YUMOTO, QG-U and NUZ cell lines, were maintained as monolayer cultures in Ham's F-12 medium (Flow Laboratories Inc., Irvine, Scotland) supplemented with 10% fetal bovine serum (Mitsubishi Chemical Co., Tokyo) at 37°C in a humidified incubator with 5% CO_2 in air. The YUMOTO, QG-U and NUZ cell lines were cultured in RPMI-1640 medium (GIBCO BRL, Bethesda, MD) supplemented with 10% fetal bovine serum as described above. The cells were grown in 75-cm^2 tissue culture flasks (Nunc, Roskilde, Denmark), washed with phosphate-buffered saline (PBS) and then harvested after a brief treatment with 0.1% trypsin solution containing 0.02% EDTA (Flow). The cell viability was determined by trypan blue dye exclusion prior to use.

Protein solution of cervical carcinoma cells was prepared from each cell line as previously described [30]. Briefly, confluent monolayers of tumor cells grown in 10 cm plastic dishes (Corning 25010, Iwaki Glass, Tokyo) were rinsed twice with cold PBS and then lysed with modified RIPA buffer (2 mM sodium orthovanadate, 50 mM NaF, 20 mM HEPES, 150 mM NaCl, 1.5 mM $MgCl_2$, 5 mM sodium pyrophosphate, 10% glycerol, 0.2% Triton X 100, 5 mM EDTA, 1 mM PMSF, 10 mg/ml leupeptin and 10 mg/ml aprotinin). The protein concentration of each sample was determined by using a DC protein Assay Kit (BioRad Laboratories, Hercules, CA) and then stored at −80°C until use.

Tissue sample

Normal cervical tissues were obtained from 14 women who received hysterectomy under the diagnosis of uterine myoma and were used for mRNA analysis with consent. These tissues did not have any findings of cervical neoplasms and consisted of normal epithelial and stromal components, which was confirmed by pathological observation. Gene expression levels of these materials containing both components were evaluated in total as previously described by Van Trappen et al. [19]. All tissue samples were immediately frozen in liquid nitrogen and then stored at −80°C until use.

RNA isolation and cDNA preparation

RNA was extracted from cell lines and homogenized tissue samples by a combination of initial phenol/chloroform extraction according to the RNA STAT-60 protocol (Tel-Test, Inc, Friendswood, TX) and then SV-total RNA isolation kit extraction (Promega Corp, Madison, WI) according to the supplier's recommendation. Contaminating residual genomic DNA was removed by digestion with RNase free DNase (Promega). cDNAs were prepared using at least 2 μg of total RNA and SUPERSCRIPT II reverse transcriptase (GIBCO BRL Life Technologies, Gaithersburg, MD) with random hexamers as primers and were finally dissolved in diethyl pyrocarbonate-treated water and then frozen at −20°C until use.

Quantitative reverse transcription (RT)-PCR analysis

Quantitative PCR amplification was performed with a LightCycler (Roche Diagnostics, Tokyo, Japan) according to the method reported by Yamada et al. [31] with some modifications for each target gene. As an internal control, the expression of β-actin mRNA was measured. The primer pairs and hybridization probes for total VEGF-A, VEGF-A splicing variants ($VEGF_{121}$, $VEGF_{165}$ and $VEGF_{189}$), VEGF-B, C and D, bFGF, dThdPase, MMP-2, uPA and β-actin are shown in Table 1. Two microliters of cDNA aliquots was subjected to amplification in a 20 μl reaction mixture containing 2 μl LightCycler-FastStart Mix (Taq DNA polymerase, reaction buffer and deoxynucleoside triphosphate mix; Roche Molecular Biochemicals, Mannheim, Germany), 1 μl sense and antisense primers (10 pM), 1 μl hybridization probe R (8 pM), 1 μl hybridization probe F (4 pM), 3 mM $MgCl_2$ and sterile distilled water. After an initial denaturation at 95°C for 15 min, 40 cycles of denaturation at 95°C for 10 s, annealing at 62°C for 10 s and extension at 72°C for 10 s for the respective target genes were carried out on a Roche LightCycler System. A standard curve was generated using fluorescent data from the serial dilutions of the plasmid including a single PCR product for each gene. The gene expression levels were expressed as 1000 × each target gene/β-actin. Each analysis was performed in triplicate.

Sandwich enzyme-linked immunosorbent assay (sandwich ELISA) for VEGF-C and MMP-2

Protein solution of each cell line was assayed for VEGF-C expression of tumor cells according to the method reported by Weich et al. [32] with some modifications. Briefly, 10 μg/ml of anti-human VEGF-C rabbit IgG 103 (IBL, Gunma, Japan) was used for coating, and the antigen-affinity purified and horseradish-peroxidase (HRP)-conjugated antibody 408 (IBL) at 1 μg/ml was used as a detector antibody. As a standard, recombinant human VEGF-C (IBL) was used over a concentration range between 0.1 and 6.25 ng/ml. For visualization of the detector, tetra-methylbenzidine (Roche, Mannheim, Germany) was used. After stopping the reaction with 1 M H_2SO_4, the absorbance was measured at 450 nm by a microplate reader (Tosoh model MPR-A4, Tokyo). Generally, the samples were analyzed in different dilutions, measuring each dilution in triplicate.

MMP-2 expression of tumor cells was assayed according to the method reported by Fujimoto et al. [33]. A protein solution containing MMP-2 was mixed with 50 μg/l anti-MMP-2 IgG (clone 43-3F9, Fuji, Toyama, Japan)–HRP conjugate in 10 mM sodium phosphate buffer (pH 7.0) containing 10 g/l bovine serum albumin, 0.1 M NaCl and 10 mM EDTA; 0.1 ml aliquots of the mixture was transferred to each microplate well previously coated with an anti-MMP-2 IgG (clone 75-7F7, Fuji). As a standard, purified human MMP-2 (Fuji) was used. HRP activity

Table 1
Primers/probes sequences used in the real-time quantitative RT-PCR assays for 11 genes involved in angiogenesis and tumor invasion and the housekeeping gene β-actin

Genes	Sense primers	Antisense primers	Hybridization probe F	Hybridization probe R
VEGF-A total	5′-CCCTGATGAGATCGAGTACATCTT-3′	5′-ACCGCCTCGGCTTGTCAC-3′	ACTGAGGAGTCCAACATCACCATGCA	ATTATGCGGATCAAACCTCACCAAGG
121	5′-CCCTGATGAGATCGAGTACATCTT-3′	5′-GCCTCGGCTTGTCACATTTT-3′	ACTGAGGAGTCCAACATCACCATGCA	ATTATGCGGATCAAACCTCACCAAGG
165	5′-CCCTGATGAGATCGAGTACATCTT-3′	5′-AGCAAGGCCCACAGGATTT-3′	ACTGAGGAGTCCAACATCACCATGCA	ATTATGCGGATCAAACCTCACCAAGG
189	5′-CCCTGATGAGATCGAGTACATCTT-3′	5′-AACGCTCCAGGACTTATACCG-3′	ACTGAGGAGTCCAACATCACCATGCA	ATTATGCGGATCAAACCTCACCAAGG
VEGF-B	5′-TGACATCACCCATCCCACTC-3′	5′-CACCCTGCTGAGTCTGAAAA-3′	GGGCTTAGAGCTCAACCCAGACACCT	CAGGTGCCGGAAGCTGCGAA
VEGF-C	5′-CCAGAAATCAACCCCTAAAT-3′	5′-AATATGAAGGGACACAACGA-3′	GTTCCACCACCAAACATGCAGC	GTTACAGACGGCCATGTACGAACC
VEGF-D	5′-TTCACACCAGCTAAGGAGTC-3′	5′-AGTTTTCCTCATCTGCTCTG-3′	TCCTCTCCATTCCTTGGTGCGC	GAGGCATCTGCAGCTAGAAGACATCCAT
bFGF	5′-AAGAAGAGGAAGTCACAGAA-3′	5′-TAAGGGAAGTCAGCATGTAA-3′	CAGGGGATGGGTAAGACAGTCTATGGTAA	ACAGTCTACAGTCACAGCACATGGGAATT
dThdPase	5′-AATGTCATCCAGAGCCCAGA-3′	5′-TCCGAACTTAACGTCCACCA-3′	GAGATGTGACAGCCACCGTGGACAG	CTGCCACTCATCACAGCCTCCATTC
MMP-2	5′-GTGGATGCCGCCTTTAACTG-3′	5′-AGCAGCCTAGCCAGTCGGAT-3′	GCTTTCCCAAGCTCATCGCAGATG	CTGGAATGCCATCCCCGATAACCT
uPA	5′-CTGAAGTCACCACCAAAATG-3′	5′-ATCCAGGGTAAGAAGTGTGA-3′	TTCCCTCCAAGGCCGCATGACT	TGACTGGAATTGTGAGCTGGGGC
β-actin	5′-CCAACCGCGAGAAGATGAC-3′	5′-GGAAGGAAGGCTGGAAGAGT-3′	CCTCCCCCATGCCATCCTGCGTC	GGACCTGGCTGGCCGGGACCTGA

bound on the plate was assayed by adding 100 μl of 0.15 M citric acid–sodium phosphate buffer containing 2.0 g/l o-phenylenediamine and 0.02% H_2O_2. After stopping the reaction with 1 M H_2SO_4, the absorbance was measured at 492 nm by a microplate reader. Each assay was performed in triplicate.

Haptoinvasion assay

The invasive activity of tumor cells was assayed in Chemotaxicell culture chambers (Kurabo, Osaka) according to the method reported by Albini et al. [34] with some modifications as previously described [35]. Polyvinylpyrroridone-free polycarbonate filters with 8.0 μm pore size were precoated with 10 μg of fibronectin in a volume of 50 μl of PBS on the lower surface and dried overnight at room temperature under a hood. The Matrigel diluted to 500 μg/ml with cold PBS was then applied to the upper surface of the filters (5 μg/filter) and dried again. Log-phase cell cultures of tumor cells were harvested with 0.1% trypsin containing 0.02% EDTA and resuspended to a final concentration of 3.0×10^6/ml in growth medium. 200 μl of cell suspension was added to the upper compartment, and 600 μl of growth medium was immediately added to the lower compartment. The chambers were then incubated for 24 h at 37°C in a 5% CO_2 air. The filters were fixed with ethanol and stained with hematoxylin. The cells on the upper surface of the filters were removed by wiping with a cotton swab. The cells that had migrated to various areas of the lower surface were manually counted under a microscope at a magnification of 400. Each assay was performed in triplicate.

Statistical analysis

All statistical calculations were carried out using StatView statistical software. The Spearman rank correlation coefficient was used to analyze the relation between two different values. The Mann–Whitney U test was used to compare the gene expression levels between normal and malignant cell samples. A level of $P < 0.05$ was accepted as statistically significant.

Results

Gene co-expression patterns in cervical carcinoma cells and normal cervical tissues

Real-time quantitative RT-PCR analysis was performed on mRNA transcripts of 11 genes (total VEGF-A, $VEGF_{121}$, $VEGF_{165}$, $VEGF_{189}$, VEGF-B, C and D, bFGF, dThdPase, MMP-2 and uPA) involved in angiogenesis and tumor invasion. Tables 2 and 3 show the Spearman correlation matrices of gene co-expression patterns with coefficient correlation (rho) and P values in cervical carcinoma cells and normal cervical tissues, respectively. In malignant cervical cells, significant co-expressions were found among total VEGF-A and different VEGF-A splicing variants. VEGF-B was also co-expressed with VEGF-A. There were statistically significant correlations in gene expression levels between $VEGF_{165}$ and dThdPase or VEGF-C and MMP-2. Significant co-expressions were also observed between uPA and VEGF-A or MMP-2. There were no statistical differences in gene expression levels of various angiogenic

Table 2
Spearman correlation matrix to assess gene co-expression (with rho and P values) in cervical carcinoma cells

		$VEGF_{total}$	$VEGF_{121}$	$VEGF_{165}$	$VEGF_{189}$	VEGF-B	VEGF-C	VEGF-D	bFGF	dThdPase	MMP-2	uPA
$VEGF_{total}$	rho	1.000										
	P value											
$VEGF_{121}$	rho	0.951	1.000									
	P value	<0.0001										
$VEGF_{165}$	rho	0.972	0.909	1.000								
	P value	<0.0001	<0.0001									
$VEGF_{189}$	rho	0.965	0.916	0.909	1.000							
	P value	<0.0001	<0.0001	<0.0001								
VEGF-B	rho	0.713	0.664	0.797	0.664	1.000						
	P value	0.009	0.018	0.002	0.018							
VEGF-C	rho	0.368	0.291	0.406	0.403	0.123	1.000					
	P value	0.240	0.359	0.190	0.194	0.704						
VEGF-D	rho	−0.051	0.087	−0.094	−0.029	−0.022	−0.458	1.000				
	P value	0.876	0.788	0.771	0.929	0.946	0.135					
bFGF	rho	0.259	0.119	0.308	0.252	0.357	−0.070	0.051	1.000			
	P value	0.417	0.713	0.331	0.430	0.255	0.829	0.876				
dThdPase	rho	0.483	0.448	0.580	0.503	0.483	0.574	−0.392	0.028	1.000		
	P value	0.112	0.145	0.048	0.095	0.112	0.051	0.208	0.931			
MMP-2	rho	0.345	0.373	0.303	0.465	0.070	0.635	−0.190	−0.063	0.359	1.000	
	P value	0.272	0.232	0.339	0.128	0.828	0.027	0.555	0.845	0.252		
uPA	rho	0.644	0.683	0.588	0.764	0.518	0.311	−0.123	0.235	0.508	0.713	1.000
	P value	0.024	0.014	0.044	0.004	0.084	0.326	0.702	0.463	0.092	0.009	

Table 3
Spearman correlation matrix to assess gene co-expression (with rho and *P* values) in normal cervical tissues

		$VEGF_{total}$	$VEGF_{121}$	$VEGF_{165}$	$VEGF_{189}$	VEGF-B	VEGF-C	VEGF-D	bFGF	dThdPase	MMP-2	uPA
$VEGF_{total}$	rho	1.000										
	P value											
$VEGF_{121}$	rho	0.231	1.000									
	P value	0.471										
$VEGF_{165}$	rho	0.657	0.322	1.000								
	P value	0.020	0.308									
$VEGF_{189}$	rho	0.687	−0.288	0.434	1.000							
	P value	0.014	0.363	0.158								
VEGF-B	rho	0.413	0.175	0.308	0.214	1.000						
	P value	0.183	0.587	0.331	0.505							
VEGF-C	rho	−0.266	0.559	0.021	−0.363	−0.021	1.000					
	P value	0.404	0.059	0.948	0.246	0.948						
VEGF-D	rho	−0.341	−0.470	−0.433	−0.112	0.233	−0.054	1.000				
	P value	0.278	0.123	0.160	0.728	0.466	0.867					
bFGF	rho	−0.130	−0.063	−0.035	−0.337	0.522	0.112	0.458	1.000			
	P value	0.688	0.846	0.914	0.284	0.082	0.729	0.134				
dThdPase	rho	0.573	0.615	0.308	0.014	0.392	0.084	−0.387	−0.049	1.000		
	P value	0.051	0.033	0.331	0.965	0.208	0.795	0.214	0.880			
MMP-2	rho	0.294	−0.056	0.287	0.320	0.552	0.280	0.420	0.340	0.042	1.000	
	P value	0.354	0.863	0.366	0.310	0.063	0.379	0.174	0.280	0.897		
uPA	rho	−0.301	0.266	−0.308	−0.036	−0.056	0.406	−0.108	−0.102	0.063	−0.301	1.000
	P value	0.342	0.404	0.331	0.913	0.863	0.191	0.738	0.753	0.846	0.342	

factors and proteinases between squamous and adenocarcinoma cell lines. In normal cervical tissues, total VEGF-A was co-expressed with $VEGF_{165}$ or $VEGF_{189}$. Gene expression levels of $VEGF_{121}$ were also statistically correlated with those of dThdPase. However, gene co-expression was not observed among other angiogenic factors and proteinases.

Correlation between VEGF-C or MMP-2 expression and invasive phenotype in cervical carcinoma cells

We then investigated the relationship between VEGF-C or MMP-2 expression and in vitro invasive activity of tumor cells estimated by haptoinvasion assay. As shown in Figs. 1A and B, there was a statistically significant correlation between VEGF-C gene or protein expression and the number of invaded tumor cells, with a coefficient correlation of 0.917 ($P < 0.0001$) and 0.912 ($P < 0.0001$), respectively. Gene or protein expression levels of MMP-2 in 11 cultured cervical carcinoma cells were also well correlated with the number of invaded tumor cells (Figs. 1C and D), with a coefficient correlation of 0.671 ($P = 0.0238$) and 0.723 ($P = 0.0120$), respectively. However, there was no statistical correlation between mRNA expression levels of the other genes and invasive activity of the cells.

Differences in transcript levels of the genes in normal cervical tissues and malignant cervical cells

Fig. 2 illustrates the transcript levels in normal cervical tissues and malignant cervical cells for 11 genes involved in angiogenesis and tumor invasion. All normal and malignant cervical samples expressed various angiogenic factors and proteinases examined. The gene expression levels of different VEGF-A splicing variants were significantly higher in malignant compared to benign samples ($P < 0.01$). In contrast, there was no statistical difference in mRNA expression levels of VEGF-B, C and D between normal cervical tissues and cervical carcinoma cells. The levels of MMP-2 in malignant were higher than those in benign samples ($P < 0.05$), however, no statistical difference was found in bFGF, dThdPase or uPA gene expression between two groups.

Discussion

Various kinds of genes have now been identified which are involved in both tumor neovascularization and invasion, and most of them are also expressed to some extent under normal physiologic conditions. In the present study, combined analysis of real-time quantitative RT-PCR with correlation matrices of gene expression data revealed the differences in gene co-expression patterns between malignant and normal cervical samples. In cervical carcinoma cells, significant co-expressions were found among total VEGF-A and VEGF-A splicing variants ($VEGF_{121}$, $VEGF_{165}$ or $VEGF_{189}$), which is consistent with the previous reports [19]. Moreover, VEGF-B was also co-expressed with VEGF-A. VEGF-A binds with high affinity to two tyrosine kinase receptors on the cell membrane of vascular endothelial cells; VEGF receptor (VEGFR)-1 (Flt-1) and VEGFR-2 (KDR/Flk-1). Binding of VEGF-A causes receptor dimerization followed by autophosphorylation of the receptor and signal transduction [2,3]. VEGF-

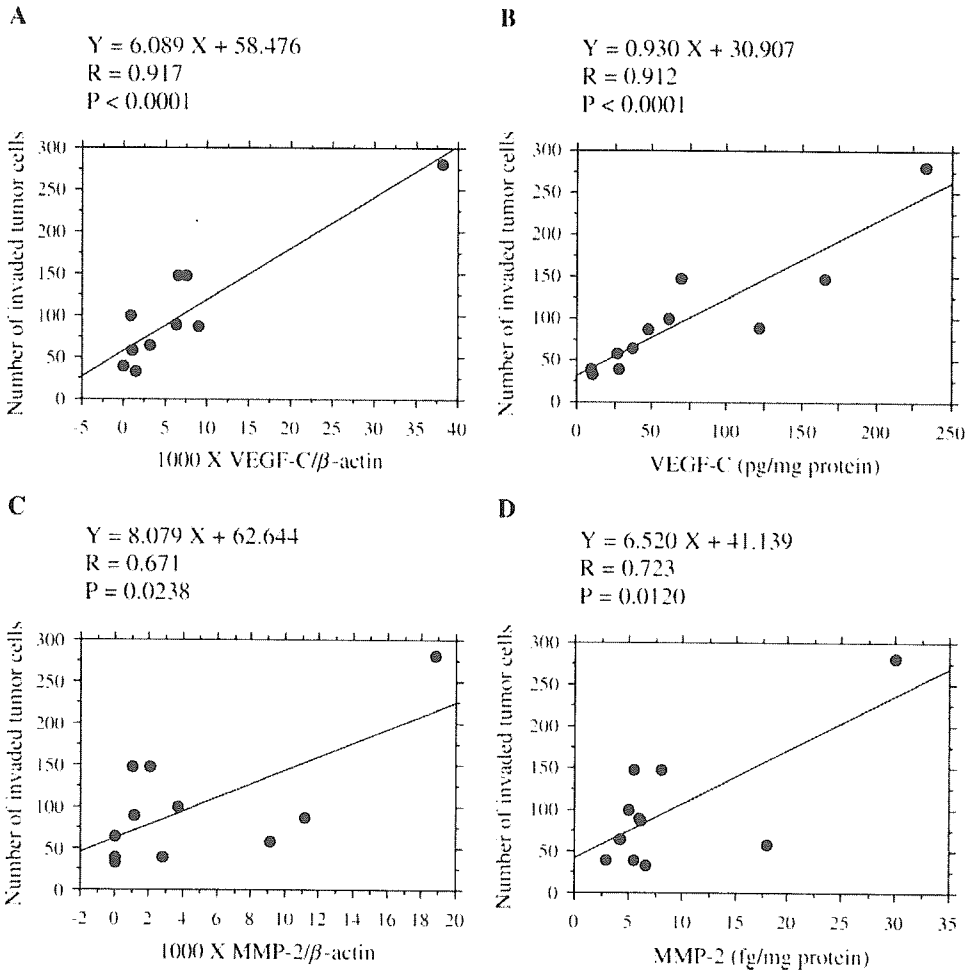

Fig. 1. Correlation between VEGF-C gene or protein expression and the number of invaded tumor cells (A or B) and between MMP-2 gene or protein expression and the number of invaded tumor cells (C or D), respectively. Each point represents the mean of triplicates for each cell line.

B, one of the new VEGF family members, also binds to Flt-1 and induces pleiotropic responses of endothelial cells [11]. The gene co-expression pattern of VEGF-A and B may suggest their cooperative role for tumor angiogenesis. Our present results further demonstrated statistical correlations in gene expression levels between $VEGF_{165}$ and dThdPase, VEGF-C and MMP-2, or uPA and VEGF-A or MMP-2. Recent studies have reported that tumors exhibiting higher expression levels of VEGF-A or VEGF-C possess a higher metastatic potential [36–38]. dThdPase expression is also considered to be strongly linked to the process of tumor invasion and metastasis [35,39]. The gene expression of angiogenic factors may be closely associated with proteolytic and invasive properties of cervical carcinoma cells. In contrast, there was no statistical correlation in gene expression levels between angiogenic factors and proteinases in normal cervical tissues. Although gene co-expression was observed among total VEGF-A, VEGF-A splicing variants and dThdPase, angiogenesis may not be related to ECM degradation by proteolytic enzymes in normal physiologic conditions.

We next examined the correlation between gene expression levels of angiogenic factors and proteinases and in vitro invasive activity of cervical carcinoma cells. Interestingly, VEGF-C and MMP-2 gene expression was closely associated with the number of invaded tumor cells. Moreover, their protein expression was also well correlated with invasive activity of the cells. VEGF-C is a ligand for VEGFR-3 (Flt-4), a tyrosine kinase receptor which is predominantly expressed in the endothelium of lymphatic vessels [10]. Experimental results with the VEGF-C-transgenic mouse have shown that VEGF-C expression is associated with hyperplasia of lymphatic vessels [40]. Thus, VEGF-C is ranked first as a lymphoangiogenic factor, which induces lymphatic proliferation and spread of solid tumors. Recently, some investigators have demonstrated the close correlation between VEGF-C expression and lymphatic invasion and lymphnode metastasis in a variety of human malignant tumors [41–43]. Moreover, it is generally accepted that tumor cell invasion into the lymphatic vessels is established by the destruction of stroma around the lymphatic vessels via activation of matrix-digesting

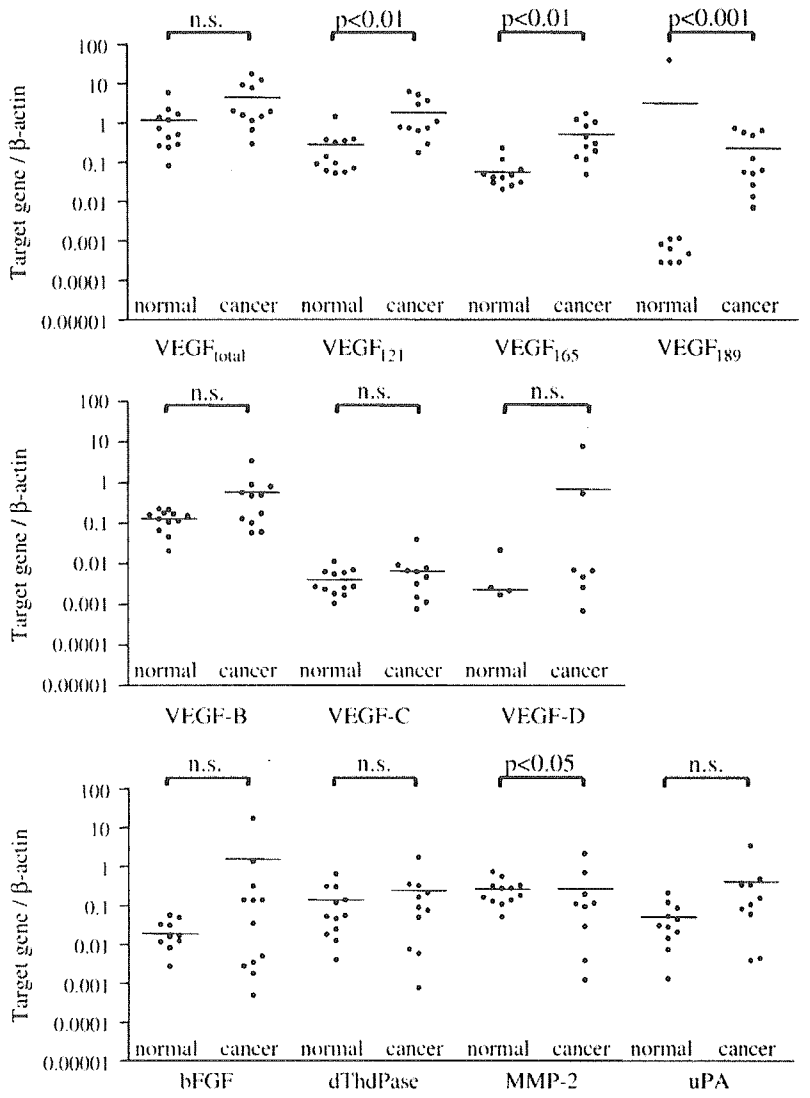

Fig. 2. Transcript levels (target gene/β-actin) of the genes implicated in angiogenesis and tumor invasion in normal cervical tissues and cultured cervical carcinoma cells. Each point represents the mean of triplicates for each tissue sample or cell line. Bars, median values.

enzymes, which are produced by tumor cells or fibroblasts [44]. Therefore, it could be expected that VEGF-C expression in tumor cells is linked to invasive phenotype of the cells. Our experimental results on the correlation among VEGF-C, MMP-2 and invasiveness suggest that cervical carcinoma cells producing VEGF-C may have a higher invasive and metastatic potential because of their capacity to pass through tissue barriers by degrading ECM with MMP-2.

Finally, we compared the transcript levels of angiogenic factors and proteinases between normal cervical tissues and cultured cervical carcinoma cells. The gene expression levels of different VEGF-A splicing variants and MMP-2 were higher in malignant compared to benign samples, however, no statistical difference was found in other genes examined. Van Trappen et al. [19] reported that VEGF-A isoforms ($VEGF_{121}$ and $VEGF_{165}$), VEGF-C and MMP-9 gene expression were significantly increased in malignant compared to normal cervical tissues and that there was no significant difference in mRNA expression levels of $VEGF_{189}$, bFGF and MMP-2 between two groups. They used malignant cervical tissue samples surgically obtained from the patients. The discrepancy might be due to the differences of materials and culture conditions. It has been demonstrated that VEGF-A is essential for the initial but not for continued growth of human breast carcinomas and that other angiogenic factors can substitute for VEGF-A during disease progression [45]. In the present study, transcript levels of VEGF-A splicing variants were increased in cervical carcinoma cells compared to normal cervical tissues but not associated with the invasive activity of tumor cells as described above. VEGF-A isoforms might be involved in the process leading to the transformation of normal cervical cells rather than in the development of cervical carcinomas.

In conclusion, gene co-expression analysis revealed the significant correlation between angiogenic factors and proteinases in cervical carcinoma cells but not in normal cervical tissues. Among the genes examined, VEGF-C and MMP-2 were closely related to invasive phenotype of tumor cells, whereas VEGF-A isoforms were considered to be involved in cervical carcinogenesis. Further studies are needed to clarify the molecular events that coregulate the genes implicated in angiogenesis and tumor invasion.

Acknowledgments

The authors are grateful to Dr. S. Nozawa, Keio University, Tokyo, Dr. N. Tanaka, Chiba University, Chiba, Dr. I. Ishiwata, Ishiwata Hospital, Mito and Dr. O. Hayakawa, Sapporo Medical College, Sapporo for the gift of cervical carcinoma cell lines. We also thank E. Shintani and K. Sato for their technical assistance. This work was supported in part by High-Tech Research Program of Osaka Medical College.

References

[1] Folkman J. Clinical applications of research on angiogenesis. N Engl J Med 1995;333:1757–63.
[2] Connolly DT. Vascular permeability factor: a unique regulator of blood vessel function. J Cell Biochem 1991;47:219–23.
[3] Shweiki D, Neeman M, Itin A, Keshet E. Induction of vascular endothelial growth factor expression by hypoxia and by glucose deficiency in multiple spheroids: implications for tumor angiogenesis. Proc Natl Acad Sci U S A 1995;92:768–72.
[4] Kandel J, Bassy-Wetzel E, Radvanyi F, Klagsburn M, Folkman J, Hanahan D. Neovascularization is associated with a switch to the export of b-FGF in the multistep development of fibrosarcoma. Cell 1991;66:1095–104.
[5] Ohtani H, Nakamura S, Watanabe Y, Mizoi T, Saku T, Nagura H. Immunocytochemical localization of basic fibroblast growth factor in carcinomas and inflammatory lesions of the human digestive tract. Lab Invest 1993;68:520–7.
[6] Furukawa T, Yoshimura A, Sumizawa T, Haraguchi M, Akiyama S. Angiogenic factor. Nature (London) 1992;356:668.
[7] Haraguchi M, Miyadera K, Uemura K, Sumizawa T, Furukawa T, Yamada K, et al. Angiogenic activity of enzymes. Nature (London) 1994;368:198.
[8] Moghaddam A, Zhang HT, Fan TPD, Hu DE, Lees VC, Turley H, et al. Thymidine phosphorylase is angiogenic and promotes tumor growth. Proc Natl Acad Sci U S A 1995;92:998–1002.
[9] Veikkola T, Alitalo K. VEGFs, receptors and angiogenesis. Semin Cancer Biol 1999;9:211–20.
[10] Yancopoulos GD, Davis S, Gale NW, Rudge JS, Wiegand SJ, Holash J. Vascular-specific growth factors and blood vessel formation. Nature 2000;407:242–8.
[11] Olofsson B, Pajusola K, Kaipainen A, von Euler G, Joukov V, Saksela O, et al. Vascular endothelial growth factor B, a novel growth factor for endothelial cells. Proc Natl Acad Sci U S A 1996;93:2576–81.
[12] Joukov V, Pajusola K, Kaipainen A, Chilov D, Lahtinen I, Kukk E, et al. A novel vascular endothelial growth factor, VEGF-C, is a ligand for the Flt4 (VEGFR-3) and KDR (VEGFR-2) receptor tyrosine kinase. EMBO J 1996;15:290–8.
[13] Achen MG, Jeltsch M, Kukk E, Makinen T, Vitali A, Wilks AF, et al. Vascular endothelial growth factor D (VEGF-D) is a ligand for the tyrosine kinases VEGF receptor 2 (Flk1) and VEGF receptor 3 (Flt4). Proc Natl Acad Sci U S A 1998;95:548–53.
[14] Liotta LA, Steeg PS, Stetler-Stevenson WG. Cancer metastasis and angiogenesis: an imbalance of positive and negative regulation. Cell 1991;64:327–36.
[15] Woessner JFJ. Matrix metalloproteinases and their inhibitors in connective tissue remodeling. FASEB J 1991;5:2145–54.
[16] Liotta LA, Rao CV, Barsky SH. Tumor invasion and the extracellular matrix. Lab Invest 1983;49:636–49.
[17] Dano K, Andreasen PA, Grondahl-Hansen J, Kristensen P, Nielsen LS, Skriver L. Plasminogen activators, tissue degradation and cancer. Adv Cancer Res 1985;44:139–266.
[18] Weidner N, Semple JP, Welch WR, Folkman J. Tumor angiogenesis and metastasis-correlation in invasive breast carcinoma. N Engl J Med 1991;324:1–8.
[19] Van Trappen PO, Ryan A, Carroll M, Lecoeur C, Goff L, Gyselman VG, et al. A model for co-expression pattern analysis of genes implicated in angiogenesis and tumour cell invasion in cervical cancer. Brit J Cancer 2002;87:537–44.
[20] Ueda M, Ueki M, Yamada T, Okamoto Y, Maeda T, Sugimoto O, et al. Scatchard analysis of EGF receptor and effects of EGF on growth and TA-4 production of newly established uterine cervical cancer cell line (OMC-1). Hum Cell 1989;2:401–10.
[21] Ueda M, Ueki M, Sugimoto O. Characterization of epidermal growth factor (EGF) receptor and biological effect of EGF on human uterine cervical adenocarcinoma cell line OMC-4. Hum Cell 1993;6:218–25.
[22] Taguchi S. Establishment and characterization of the human uterine cervical epidermoid cancer cell line. Acta Obstet Gynecol Jpn 1981; 33:1180–8.
[23] Ishiwata I, Nozawa S, Kiguchi K, Kurihara S, Okumura H. Establishment of human uterine cervical cancer cell line and comparative studies between normal and malignant uterine cervical cells in vitro. Acta Obstet Gynaecol Jpn 1978;30:731–8.
[24] Nozawa S, Udagawa Y, Ohta H, Kurihara S, Fishman WH. Newly established uterine cervical cancer cell line (SKG-III) with Regan isoenzyme, human chorionic gonadotropin β-subunit, and pregnancy-specific β1-glycoprotein phenotypes. Cancer Res 1983;43:1748–60.
[25] Mitsuhashi A, Tanaka H, Tanaka N, Sugita M, Shirasawa H, Tokita H, et al. Establishment and characterization of a new HPV-negative squamous cell carcinoma cell line (Yumoto) from the human uterine cervix. Gynecol Oncol 1998;70:339–47.
[26] Shirasawa H, Tomita Y, Fuse A, Yamamoto T, Tanzawa H, Sekiya S, et al. Structure and expression of an integrated human papillomavirus type 16 genome amplified in a cervical carcinoma cell line. J Gen Virol 1989;70:1913–9.
[27] Suzumori K, Yasui Y. NUZ-1. Hum Cell 1988;1:454.
[28] Ishiwata I, Ishiwata C, Soma M, Ono I, Nakaguchi T, Nozawa S, et al. Differences between cell lines of uterine cervical glassy cell carcinoma and large cell nonkeratinizing squamous cell carcinoma. Anal Quant Cytol Histol 1990;12:290–8.
[29] Koizumi M, Uede T, Shijubo N, Kudo R, Hashimoto M, Kikuchi K. New monoclonal antibody, 1C5, reactive with human cervical adenocarcinoma of the uterus, with immunodiagnostic potential. Cancer Res 1988;48:6565–72.
[30] Terai Y, Abe M, Miyamoto K, Koike M, Yamasaki M, Ueda M, et al. Vascular smooth muscle cell growth-promoting factor/F-spondin inhibits angiogenesis via the blockade of integrin αVβ3 on vascular endothelial cells. J Cell Physiol 2001;188:394–402.
[31] Yamada Y, Kuroiwa T, Nakagawa T, Kajimoto Y, Dohi T, Azuma H, et al. Transcriptional expression of survivin and its splice variants in brain tumors in humans. J Neurosurg 2003;99:738–45.
[32] Weich HA, Bando H, Brokelmann M, Baumann P, Toi M, Barleon B, et al. Quantification of vascular endothelial growth factor-C (VEGF-C) by a novel ELISA. J Immunol Methods 2004;285:145–55.
[33] Fujimoto N, Mouri N, Iwata K, Ohuchi E, Okada Y, Hayakawa T. A one-step sandwich enzyme immunoassay for human matrix metal-

loproteinase 2 (72-kDa gelatinase/type IV collagenase) using monoclonal antibodies. Clin Chim Acta 1993;221:91–103.
[34] Albini A, Iwamoto Y, Kleinman HK, Martin GR, Aaronson SA, Kozlowski JM, et al. A rapid in vitro assay for quantitating the invasive potential of tumor cells. Cancer Res 1987;47:3239–45.
[35] Ueda M, Terai Y, Kumagai K, Ueki K, Kanemura M, Ueki M. Correlation between thymidine phosphorylase expression and invasion phenotype in cervical carcinoma cells. Int J Cancer 2001;91:778–82.
[36] Potgens AJ, van Altena MC, Lubsen NH, Ruiter DJ, de Waal RM. Analysis of the tumor vasculature and metastatic behavior of xenografts of human melanoma cell lines transfected with vascular permeability factor. Am J Pathol 1996;148:1203–17.
[37] Ohta Y, Watanabe Y, Murakami S, Oda M, Hayashi Y, Nonomura A, et al. Vascular endothelial growth factor and lymph node metastasis in primary lung cancer. Br J Cancer 1997;76:1041–5.
[38] Skobe M, Hawighorst T, Jackson DG, Prevo R, Janes L, Velasco P, et al. Induction of tumor lymphangiogenesis by VEGF-C promotes breast cancer metastasis. Nat Med 2001;7:192–8.
[39] Ueda M, Terai Y, Kumagai K, Ueki K, Okamoto Y, Ueki M. Correlation between tumor angiogenesis and expression of thymidine phosphorylase, and patient outcome in uterine cervical carcinoma. Hum Pathol 1999;30:1389–94.
[40] Jetsch M, Kaipainen A, Joukov V, Meng XM, Lakso M, Rauvala H, et al. Hyperplasia of lymphatic vessels in VEGF-C transgenic mice. Science (Washington, DC) 1997;276:1423–5.
[41] Yonemura Y, Endo Y, Fujita H, Fushida S, Ninomiya I, Bandou E, et al. Role of vascular endothelial growth factor C expression in the development of lymph node metastasis in gastric cancer. Clin Cancer Res 1999;5:1823–9.
[42] Valtola R, Salven P, Heikkila P, Taipale J, Joensuu H, Rehn M, et al. VEGFR-3 and its ligand VEGF-C are associated with angiogenesis in breast cancer. Am J Pathol 1999;154:1381–90.
[43] Bunone G, Vigneri P, Mariani L, Buto S, Collini P, Pilotti S, et al. Expression of angiogenesis stimulators and inhibitors in human thyroid tumors and correlation with clinical pathological features. Am J Pathol 1999;155:1967–76.
[44] Liotta LA. Tumor invasion and metastasis: role of the extracellular matrix. Cancer Res 1986;46:1–7.
[45] Yoshiji H, Harris SR, Thorgeirsson UP. Vascular endothelial growth factor is essential for initial but not continued in vivo growth of human breast carcinoma cells. Cancer Res 1997;57:3924–8.

Int J Gynecol Cancer 2005, **15**, 224–227

Carboplatin hypersensitivity induced by low-dose paclitaxel/carboplatin in multiple platinum-treated patients with recurrent ovarian cancer

Y. WATANABE, H. NAKAI, H. UEDA, K. NOZAKI & H. HOSHIAI
Department of Obstetrics and Gynecology, Kinki University School of Medicine, Osaka, Japan

Abstract. Watanabe Y, Nakai H, Ueda H, Nozaki K, Hoshiai H. Carboplatin hypersensitivity induced by low-dose paclitaxel/carboplatin in multiple platinum-treated patients with recurrent ovarian cancer. *Int J Gynecol Cancer* 2005;15:224–227.

We report five cases of carboplatin (CBDCA) hypersensitivity after weekly low-dose paclitaxel (60 mg/m^2)/CBDCA (area under the concentration curve = 2) therapy in patients with recurrent ovarian cancer receiving multiple platinum-based chemotherapy. Paclitaxel and CBDCA therapy was indicated as second-line chemotherapy in one patient and as third line in four patients with recurrent disease. The range of previously administered total CBDCA was 2582–9589 mg, and the CBDCA area under the concentration curve of the first treatment exhibited appropriate intensity (mean, 1.92 ± 0.10; range, 1.76–2.10) in all patients. However, one patient exhibited severe hypersensitivity reactions including cardiac arrest and apnea, and another four patients developed eruptions, hypotension, and tachycardia soon after administration of CBDCA. Our report suggested that CBDCA hypersensitivity was correlated with the total dose of previously administered platinum agents and that CBDCA should be excluded in patients who have received multiple platinum-based chemotherapy, even in platinum-sensitive cases, because CBDCA hypersensitivity can occur even with low-dose CBDCA administration.

KEYWORDS: CBDCA, hypersensitivity, recurrent ovarian cancer, weekly low-dose chemotherapy.

Recent large phase-III comparative clinical trials have indicated that combination chemotherapy with carboplatin (CBDCA) and paclitaxel (TC therapy) is an effective chemoregimen for patients with advanced epithelial ovarian cancer[1]. Moreover, it has also been reported that TC therapy is effective even as a second-line therapy in recurrent epithelial ovarian cancer[2,3]. Generally, patients with advanced ovarian cancer have received multiple courses of platinum agent as first-, second-, and occasionally third-line platinum-based chemotherapy, and it is well known that the main adverse effects of platinum agents are bone marrow suppression, gastrointestinal toxicity, and neurotoxicity. Although they are rare events, previous reports[4–6] have described hypersensitivity reactions to platinum

Address correspondence and reprint requests to: Yoh Watanabe, MD, PhD, Department of Obstetrics and Gynecology, Kinki University School of Medicine, 377-2 Ohno-Higashi, Osakasayama, Osaka 589-8511, Japan. Email: watanabe@med.kindai.ac.jp

agents as an issue during multiple platinum-based chemotherapy regimens. They reported that the frequency of hypersensitivity reaction was 15% in patients receiving CBDCA for treatment every 3 weeks with the area under the concentration curve (AUC) = 5 or almost 300 mg/m^2 of CBDCA. Since 2000, we have indicated weekly paclitaxel and CBDCA therapy (WTC) with 3 weeks of administration followed by a 1-week break, for patients with recurrent epithelial ovarian cancer, as second-line chemotherapy. However, if patients requested WTC even as third-line chemotherapy, we administered this treatment under the condition that the platinum-free interval was over 6 months, to develop a therapeutic level of chemotherapy while preventing neurotoxicity under fully informed consent. We report the clinical features of those CBDCA hypersensitivity cases receiving weekly low-dose CBDCA-based chemotherapy.

Materials and methods

To begin WTC, a 60-min intravenous administration of 20 mg dexamethazone, 3 mg 5-HT$_3$ receptor antagonist, 50 mg ranitidine hydrochloride, and 50 mg of oral diphenhydramine was given before administration of paclitaxel and CBDCA. The treatment dose of paclitaxel and CBDCA was divided into three of the standard TC (paclitaxel at 180 mg/m^2, CBDCA AUC = 6): paclitaxel at 60 mg/m^2 (equal to the per-week paclitaxel dose intensity in the GOG 111[7] study), CBDCA AUC = 2 (Calvert's formula). After premedication, CBDCA was administered over 60 min followed by 60 min of paclitaxel treatment. All hypersensitivity cases had previously received platinum-based chemotherapy every 3 weeks for a total of six courses of 175 mg/m^2 paclitaxel and CBDCA AUC = 5, 500 mg/m^2 of cyclophosphamide and 70 mg/m^2 of cisplatin, or 500 mg/m^2 of cyclophosphamide and CBDCA AUC = 5 therapy. Four patients were receiving the present WTC as third-line chemotherapy, and one 72-year-old patient received this regimen as second-line chemotherapy for recurrent disease. Previously, three patients had received 18 courses of the same WTC schedule; the range of the previously administered total dose of CBDCA before hypersensitivity occurred was 2582–9589 mg, and all cases had platinum-free intervals longer than 6 months before WTC. Pretreatment performance status according to the criteria of the Eastern Cooperative Oncology Group and hematologic and nonhematologic status according to the criteria of the National Cancer Institute Common Toxicity were all within grade 1. The mean CBDCA AUC calculated by nine-point blood samples in the first opening treatment course was entirely within the approximate value (1.92 ± 0.01; range, 1.76–2.10).

Results

A total of 23 patients were treated with WTC (14 patients as second-line and nine as third-line chemotherapy). The effects of WTC for patients with recurrent ovarian cancer were 64.3% in second-line (complete response: 5, partial response: 3) and 33.3% in third-line (PR: 3) treatments, while five cases (four patients in third-line and one patient in second-line chemotherapy) developed CBDCA hypersensitivity among those receiving WTC (Table 1). All the hypersensitivity reactions occurred immediately after CBDCA administration but not during paclitaxel administration. Four patients recovered from symptoms within 10 min after stopping CBDCA administration, but one patient required respiratory assistance with intubation in an intensive care unit due to sudden apnea and cardiac arrest after fainting. Except in one patient with a severe hypersensitivity reaction, symptoms were hypotension (mean drop in blood pressure, 29 + 3 mm Hg in systolic, 14 ± 8 mm Hg in diastolic), dyspnea (mean SaO_2, 67.3 ± 3.7 cm H_2O), nausea, and eruption. Except for the one severe hypersensitivity patient, the other four patients were treated with a 2-week break after the hypersensitivity reaction with an initial 60 mg/m^2 of single paclitaxel therapy after giving the informed consent. These four patients have been able to continue treatment with more than six courses weekly of 80 mg/m^2 of single paclitaxel therapy without further hypersensitivity reactions, and two patients (one second line and one third line) achieved PR from the weekly single paclitaxel treatment. The frequency of CBDCA hypersensitivity by weekly low-dose therapy has been estimated as 44.4% (4/9) in third-line chemotherapy and 7.1% in second-line (1/14) chemotherapy.

Discussion

Primary ovarian epithelial cancer is known as a chemosensitive gynecological malignancy, and recent regimens have achieved an almost 75% overall response rate and a 40% complete response rate[1]. Therefore, patients with ovarian cancer occasionally receive multiple platinum-based chemotherapy, especially patients with a platinum-free interval of longer than 6 months. However, after multiple platinum-based chemotherapy, hypersensitivity reaction to CBDCA is a noteworthy adverse effect. Although the details of the cause remain unknown, recent studies have reported

Table 1. Characteristics of CBDCA hypersensitivity cases

Case	Age	Symptoms	Number of chemotherapy (prior regimens)	PFI	Total CBDCA (Total CDDP)	AUC of CBDCA
1	58	Eruption Hypotension Tachycardia Dyspnea	Third line (CP, TC-3)	7 months	6991 mg (1300 mg)	2.10
2	53	Eruption Hypotension Tachycardia	Third line (CC, WTC)	8 months	3780 mg	1.98
3	62	Eruption Hypotension Tachycardia	Third line (CP, WTC)	10 months	5344 mg (1036 mg)	1.92
4	72	Eruption Hypotension Tachycardia Dyspnea	Second line (TC-3)	9 months	2582 mg	1.76
5	62	Cardiac arrest Hypotension Apnea	Third line (TC-3, WTC)	15 months	9589 mg	1.81

WTC, weekly taxol (60 mg/m^2) + carboplatin (AUC = 2); CP, cyclophosphamide (500 mg/m^2) + cisplatin (70 mg/m^2); CC, cyclophosphamide (500 mg/m^2) + carboplatin (AUC = 5); TC-3, every 3 weeks taxol (175 mg/m^2) + carboplatin (AUC = 5). PFI, platinum-free interval; CBDCA, carboplatin; CDDP, cisplatin; Total CBDCA, prior total carboplatin administration before hypersensitivity; Total CDDP, prior total cisplatin administration before hypersensitivity; AUC, area under the concentration curve.

interesting facts regarding CBDCA hypersensitivity. Polyzos *et al.*[8] reported that CBDCA hypersensitivity was found in 16% and indicated that 62.5% of these cases showed mild reactions. They also reported that there was no hypersensitivity reaction in a group receiving intraperitoneal CBDCA treatment, and in 33.3% of these patients, treatment could be replaced by cisplatin. Furthermore, Robinson *et al.*[9] reported the utility of desensitization for CBDCA hypersensitivity by low-dose exposure to CBDCA. However, Markman *et al.*[4] expressed some doubts about desensitization and re-administration of platinum agents based on clinical experiences. In our cases, the mean practical weekly administered CBDCA during the course that caused a hypersensitivity reaction was 195.6 ± 26.3 mg (range, 160–260 mg), and all cases exhibited hypersensitivity reactions within 1 min after CBDCA administration (roughly estimated mean administered CBDCA dose until hypersensitivity reaction occurred was 2.17 ± 0.29 mg). Moreover, although CBDCA AUC was examined when initiating the course of WTC, the administered CBDCA AUC was confirmed as the approximate dose. Therefore, it was thought that the utility of CBDCA desensitization could not be expected because the present cases exhibited CBDCA hypersensitivity after administration of less than 2 mg of CBDCA. The incidence of CBDCA hypersensitivity after weekly low-dose CBDCA therapy remains unknown because all previous reports regarding CBDCA hypersensitivity involved a CBDCA treatment showing AUC 5–6. Yu *et al.*[10] reported that the risk of hypersensitivity in children with brain tumors treated weekly with 175 mg/m^2 of CBDCA would increase because CBDCA hypersensitivity was observed in 11.1% receiving weekly treatment and in 0.7% on the monthly schedule. However, in the present series of adult patients with recurrent ovarian cancer, hypersensitivity reaction occurred in only one elderly patient receiving second-line chemotherapy, and the frequency of hypersensitivity was increased in third-line chemotherapy. These results suggest that the risk of CBDCA hypersensitivity is not correlated to a definite amount or administration schedule but to the prior accumulated dose of the CBDCA. Moreover, it was also suggested that CBDCA hypersensitivity could be considered as platinum toxicosis because all the patients showed hypersensitivity reaction after administration of premedication, including dexamethazone for preventing allergic reactions. Although the efficacy of third-line chemotherapy for patients with recurrent ovarian cancer has not been established, the present report suggests that WTC is a safe treatment regimen as second-line chemotherapy for such patients after considering the risk of CBDCA hypersensitivity. Moreover, it remains unknown whether the pretreatment dose of CDDP affects CBDCA hypersensitivity and how much CBDCA will influence the hypersensitivity reaction because five out of nine (55.6%) patients who received third-line WTC treatment did not sustain CBDCA hypersensitivity even

though they received full courses of WTC. However, consideration should be given to the fact that among the present CBDCA hypersensitivity cases, four patients (80.0%) were receiving WTC as third-line chemotherapy and three (60.0%) had previously received over 5000 mg of CBDCA. Therefore, intensive observation is necessary during CBDCA-based chemotherapy in such patients. Furthermore, exclusion of CBDCA might be recommended in patients who have already received multiple platinum-based chemotherapies, for treatment safety, even if the patients are identified as platinum sensitive.

References

1 du Bois A, Luck HJ, Meier W *et al.* Carboplatin/paclitaxel versus cisplatin/paclitaxel as first-line chemotherapy in advanced ovarian cancer: an interim analysis of a randomized phase III trial of the Arbeitsgemeinschaft Gynecologishe Onkologie Ovarian Cancer Group. *Semin Oncol* 1997;**24**:44–52.

2 Dizon DS, Hensley ML, Poynor EA *et al.* Retrospective analysis of carboplatin and paclitaxel as initial second-line therapy for recurrent epithelial ovarian carcinoma: application toward a dynamic disease state model of ovarian cancer. *J Clin Oncol* 2002;**20**:1238–47.

3 The ICON and AGO Collaborators. Paclitaxel plus platinum-based chemotherapy versus conventional platinum-based chemotherapy in women with relapsed ovarian cancer: the ICON4/AGO-OVAR-2.2 trial. *Lancet* 2003; **361**:2099–106.

4 Sood AK, Gelder MS, Huang SW, Morgan LS. Anaphylaxisis to carboplatin following multiple previous uncomplicated courses. *Gynecol Oncol* 1995;**57**:131–2.

5 Markman M, Kennedy A, Webster K *et al.* Clinical features of hypersensitivity reactions to carboplatin. *J Clin Oncol* 1999;**17**:1141–5.

6 Dison DS, Sabbatini PJ, Aghajanian C, Hensley ML, Spriggs DR. Analysis of patients with epithelial ovarian cancer or fallopian tube carcinoma treated with cisplatin after the development of a carboplatin allergy. *Gynecol Oncol* 2002;**84**:378–82.

7 McGuire WP, Hoskins WJ, Brady MF *et al.* Cyclophosphamide and cisplatin versus paclitaxel and cisplatin: a phase III randomized trial in patients with suboptimal stage III/IV ovarian cancer (from the Gynecologic Oncology Group). *Semin Oncol* 1996;**23**:40–7.

8 Polyzos A, Tsavaris N, Kostama C *et al.* Hypersensitivity reactions to carboplatin administration are common but not always severe: a 10-year experience. *Oncology* 2001;**61**:129–33.

9 Robinson JB, Singh D, Bodurka-Bevers DC *et al.* Hypersensitivity reactions and the utility of oral and intravenous desensitization in patients with gynecologic malignancies. *Gynecol Oncol* 2001;**82**:550–8.

10 Yu DY, Dahl GV, Shames RS, Fisher PG. Weekly dosing of carboplatin increases risk of allergy in children. *J Pediatr Hematol Oncol* 2001;**23**:349–52.

Accepted for publication February 4, 2004

CURRENT MEDICAL RESEARCH AND OPINION®
VOL. 21, NO. 3, 2005, 363–368

0300-7995
doi:10.1185/030079905X36404

BRIEF REPORT

The effect of granisetron on *in vitro* metabolism of doxorubicin, irinotecan and etoposide

Yoh Watanabe, Hidekatsu Nakai and Hiroshi Hoshiai

Department of Obstetrics and Gynecology, Kinki University School of Medicine, Osaka, Japan

Address for correspondence: Dr Yoh Watanabe, Department of Obstetrics and Gynecology, Kinki University School of Medicine, 377-2 Ohno-Higashi, Osakasayama, Osaka 589-8511, Japan.
Tel.: +81 72366 0221; Fax: +81 72368 6874; email: watanabe@med.kindai.ac.jp

Key words: CYP3A – Doxorubicin – Etoposide – Granisetron – Irinotecan

ABSTRACT

Objective: Doxorubicin, irinotecan and etoposide are all associated with the debilitating side-effects of nausea and vomiting, thereby necessitating concomitant antiemetic therapy. However, this may increase the potential for drug–drug interactions by inhibition or induction of the cytochrome P450 enzymes. A study was undertaken to investigate the effects of the 5-HT_3-receptor antagonist granisetron on the metabolism of doxorubicin, irinotecan and etoposide *in vitro* in human liver microsomal preparations.

Research design and methods: Doxorubicin, 20 μM, irinotecan, 10 μM, and etoposide, 50 μM, were incubated in the presence of granisetron, 0 nM, 20 nM, 200 nM and 2000 nM, in human liver microsomal preparations (250 μg). The levels of unchanged doxorubicin, irinotecan and etoposide in the incubation mixture were determined by high-performance liquid chromatography. Positive controls were ketoconazole, 20 μM, a potent inhibitor of CYP3A metabolism, for irinotecan and etoposide and quercitrin, 2 mM, a potent inhibitor of aldo-keto reductase, for doxorubicin.

Results: In the absence of granisetron, unchanged doxorubicin, irinotecan and etoposide levels decreased by 34.2 ± 5.5%, 21.3 ± 2.9% and 13.4 ± 1.6% of control, respectively. Ketoconazole prevented the breakdown of both irinotecan and etoposide, while quercitrin inhibited the breakdown of doxorubicin. Granisetron had no effect on the rate of reduction of doxorubicin, irinotecan or etoposide.

Conclusions: The results from this study suggest that granisetron neither inhibits nor induces the enzymes involved in the metabolism of doxorubicin, irinotecan or etoposide. Thus, granisetron can be used safely to treat nausea and vomiting induced by these agents with minimal risk of drug–drug interactions.

Introduction

The anthracycline doxorubicin has been used for many years in combination with other cytotoxic agents for the treatment of a wide range of solid tumours and haematologic malignancies. More recently, liposomal doxorubicin has appeared as a new cytotoxic agent for the treatment of patients with advanced[1] or relapsed[2] ovarian cancer. Moreover, etoposide has been recognized as an effective agent for the treatment of lymphoma[3], metastatic testicular cancer[4], small cell lung cancer[5] and relapsed ovarian cancer[6], while irinotecan hydrate is widely used with 5-fluorouracil for the treatment of advanced colorectal cancer[7] and advanced ovarian cancer[8]. Furthermore, all these antineoplastic agents are recommended as salvage chemotherapy for relapsed epithelial ovarian cancer by the National Comprehensive Cancer Network Treatment Guidelines. However, all these agents may induce the debilitating symptoms of nausea and vomiting that are commonly associated with antineoplastic chemotherapy. Fortunately, the development of the 5-HT_3-receptor antagonists for the